RESEARCH ARTICLE | NOVEMBER 02 2022

Dynamics of chiral domain walls under applied current in cylindrical magnetic nanowires

Special Collection: Science and Technology of 3D Magnetic Nanostructures

J. A. Fernandez-Roldan ✉ ; O. Chubykalo-Fesenko

APL Mater 10, 111101 (2022)
https://doi.org/10.1063/5.0103408

Dynamics of chiral domain walls under applied current in cylindrical magnetic nanowires

Cite as: APL Mater. 10, 111101 (2022); doi: 10.1063/5.0103408
Submitted: 15 June 2022 • Accepted: 6 October 2022 •
Published Online: 2 November 2022

J. A. Fernandez-Roldan[1,2,3,a] and O. Chubykalo-Fesenko[2]

AFFILIATIONS

[1] Helmholtz-Zentrum Dresden-Rossendorf, Institute of Ion Beam Physics and Materials Research, 01328 Dresden, Germany
[2] Instituto de Ciencia de Materiales de Madrid, CSIC, 28049 Madrid, Spain
[3] Department of Physics, University of Oviedo, 33007 Oviedo, Spain

Note: This paper is part of the Special Topic on Science and Technology of 3D Magnetic Nanostructures.
[a] **Author to whom correspondence should be addressed:** j.fernandez-roldan@hzdr.de

ABSTRACT

The dynamics of two types of chiral magnetic domain walls in magnetic cylindrical nanowires under spin-polarized current are investigated by means of micromagnetic simulations. We show that Bloch point domain walls with chirality identical to that of the Oersted field can propagate without dynamical instabilities with velocities ~300 m/s. The domain wall width is shown to widen at larger current densities limiting the velocity increase. For domain walls with opposite chirality, we observed a new pinning mechanism created by the action of the Oersted field, limiting their propagation distance even after chirality switching. Vortex–antivortex domain walls transform into Bloch point domain walls, and after that they can unexpectedly propagate either along or against the direction of the current. Our findings demonstrate that domain wall dynamics under current in cylindrical magnetic nanowires can result in a plethora of different behaviors that will have important implications for future 3D spintronic devices.

I. INTRODUCTION

As nanomagnetism evolves toward the use of three-dimensional nanostructures[1–9] and toward the investigation of curvature-induced effects,[10–18] novel non-trivial magnetic textures emerge as appealing information carriers in applications based on cylindrical nanowires.[5,7,8,17,19–25] Cylindrical nanowires are one of the simplest examples of curved nanostructures with three-dimensional domain walls. These nanowires will be used as parts of 3D spintronics architectures where domain walls will serve as novel information carriers. The dynamics of domain walls in magnetic cylindrical nanowires (MCNWs) have been predicted not to suffer from the Walker breakdown phenomenon, common in magnetic stripes,[26–28] and propagation with velocities of ~1 km/s, which is above the magnonic group velocity, has been reported in micromagnetic simulations.[29]

MCNWs with typical experimental diameters (50–300 nm) present a Bloch point (BP) domain wall (DW)[20,30] configuration. This DW (previously called also vortex domain wall[31–36]) is an axially symmetric configuration as depicted in Fig. 1(a). The BPDW is expected to reach much higher velocities (~1 km/s) than those typical for stripes (~200 m/s), as required for fast recording and storage technologies.[29–31] In the center of this DW, the magnetization curls around the nanowire axis and a region between two domains contains a Bloch point. The Bloch point is the only known singularity in ferromagnets where the magnetization locally vanishes. Following the terminology used for vortices in planar dots, the rotational sense of the azimuthal (circular) component of the magnetization defines the chirality of the domain wall. The direction of the axial component is determined by the directions of the neighboring domains, either head-to-head or tail-to-tail. Importantly, Hertel *et al.* have proved that the magnetochiral dynamics of the BPDW in cylindrical nanowires and nanotubes exhibit a different response to external excitation depending on its chirality.[11,19,27] An example of a magnetochiral effect is that, under external magnetic fields of few mT, the propagation of a BPDW with a chirality parallel to natural magnetization precession sense (also called "good" chirality in literature[11]) achieves high velocities. Otherwise,

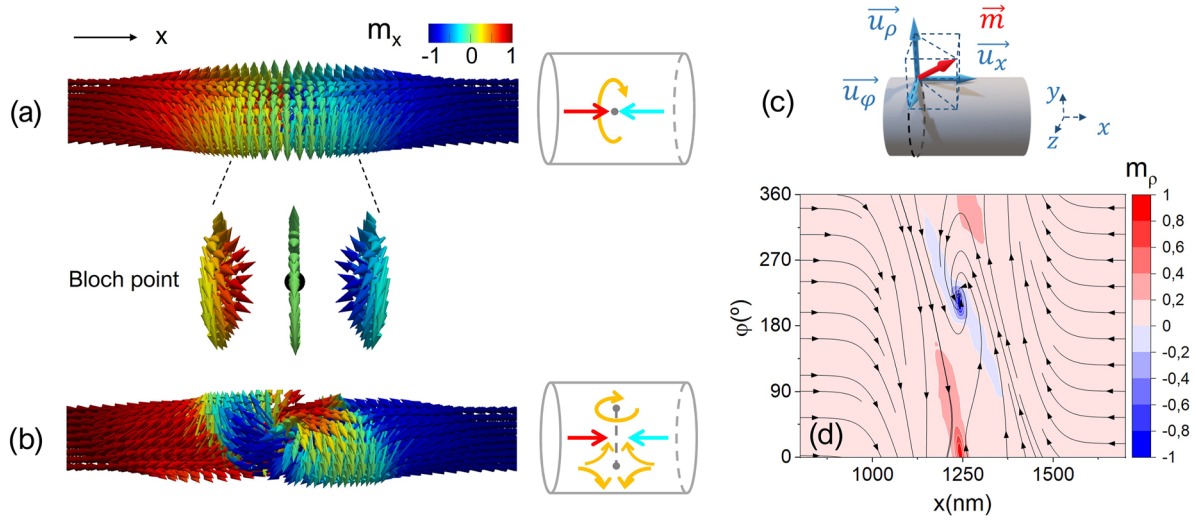

FIG. 1. (a) A head-to-head Bloch point domain wall with chirality +1 over a selection of sections showing the location of the Bloch point at the center. (b) A vortex–antivortex domain wall (VADW) from a viewpoint that enables the visualization of the vortex at the surface. (c) The lines tangent to the magnetization in the VAVDW on the unrolled nanowire surface. The color map shows the radial component and demonstrates the presence of vortex and antivortex cores with opposite polarities on the surface.

the BPDW with antiparallel chirality (also called "bad" chirality) displaces slower for higher fields (of the order of 8 mT in the particular example of Permalloy nanotube) and switches its rotational sense.

Due to the possible absence of the Walker breakdown phenomenon, BPDWs may become very appealing for spintronic applications based on cylindrical nanowires requiring fast domain wall dynamics with low current densities, i.e., energetically efficient. Since the observation of the Bloch point in cylindrical nanowires by XMCD-PEEM techniques in 2014,[20] efforts on magnetization dynamics experiment and modeling in MCNWs have increased. To our knowledge, the number of experimental studies providing measurements of DW dynamics in MCNWs is insufficient. The manipulation of chiral structures by means of currents has been experimentally confirmed in Refs. 30 and 32. Even though the BPDW existence is experimentally confirmed, it is still unclear if the cylindrical geometry permits overcoming the Walker breakdown problem because some recent results report a dynamical transformation of the BPDW into a Vortex–Antivortex (VAV) domain wall in Ni-based cylindrical nanowires[37] limiting their velocities. The VAV domain wall (also called vortex–transverse domain wall in the literature) is a non-axially symmetric configuration,[35,38] as drawn in Fig. 1(b). It consists of a chiral domain wall with the magnetization curling forming a vortex and antivortex pair on the surface of the nanowire, as shown in the unrolled magnetization in Fig. 1(c). Again, the chirality of this domain wall is determined by the curling direction of the vortex/antivortex, and it can be of the head-to-head/tail-to-tail character.

Additionally, an insufficient number of theoretical works in limited combinations of material and geometrical parameters have investigated chiral DWs and their dynamics under current.[37,39] Previous studies have used large values of the damping parameters ($\alpha \geq 0.05$ but frequently $\alpha = 1$)[37] that may affect the dynamical stability of magnetic solitons. Other works consider the dynamics of BPDW only under the Oersted field.[40] These works suggest that the Oersted field may play the dominant role in the DW dynamics under current. Previous results have also demonstrated that, even without DW, the Oersted field induces magnetization curling along the whole nanowire.[39] Furthermore, the Oersted field can switch the chirality of the BPDW to that corresponding to its rotational sense.[30,39] In our view, the DW dynamics in cylindrical nanowires have not been completely clarified so far, especially for the combined action of spin–torque transfer effect and Oersted field.

In this article, we present detailed micromagnetic modeling of the dynamics of BP and VAV domain walls under the action of an applied current that simultaneously produces an Oersted field. The main aims of this study are the following: (1) the determination of propagation direction of the DWs, (2) the evaluation of their velocities, and (3) clarifying different mechanisms of their dynamics.

II. MICROMAGNETIC MODELING OF CURRENT AND OERSTED FIELD-INDUCED WALL DYNAMICS

Due to the symmetry of the cylindrical geometry and the domain wall structures in cylindrical nanowires under spatial inversion ($x \rightarrow -x$), switching the direction of the current $\mathbf{J} \rightarrow -\mathbf{J}$ (and its respective Oersted field) is equivalent to switching the chirality of the domain wall. We have thus restricted, without loss of generality, the modeling to a single domain wall chirality, as depicted in Figs. 1(a)–1(c), and a head-to-head structure. We will call this chirality "positive" when it is parallel to the direction of the Oersted field. When the current direction is reversed, the BPDW chirality becomes antiparallel to the Oersted field direction and we will call it "negative."

We have modeled the magnetization dynamics of (1) a pre-nucleated Bloch point domain wall and (2) a pre-nucleated

TABLE I. Material parameters and crystal structure for micromagnetic modeling.

Compound	$\mu_o M_s$ (T)	A_{ex} (pJ/m)	Crystal symmetry	K_1 (kJ m^{-3})	Magnetization easy axis (e.a.)
Ni (111)	0.61	3.4	Cubic	−4.8	[111] crystal lattice direction parallel to the nanowire axis

vortex–antivortex domain wall in a 2500 nm long cylindrical Ni nanowire with a 100 nm diameter under a spin-polarized current with polarization P = 0.5, non-adiabaticity parameter ξ = 0.1, and damping parameter 0.02. Current interacts with magnetization through the Zhang–Li spin transfer torque $\boldsymbol{\tau}_{ZL}$ and the associated Oersted field following the model[39]

$$\boldsymbol{\tau}_{ZL} = \frac{1}{1+\alpha^2}\left((1+\xi\alpha)\boldsymbol{m}\times(\boldsymbol{m}\times(\boldsymbol{v}\cdot\nabla)\boldsymbol{m}) + (\xi-\alpha)\boldsymbol{m}\times((\boldsymbol{v}\cdot\nabla)\boldsymbol{m})\right), \quad (1)$$

where $\boldsymbol{v} = \frac{P\mu_B}{2e\gamma_0 M_S(1+\xi^2)}\boldsymbol{J}$, α is the magnetization damping, ξ is the degree of non-adiabaticity, μ_B is the Bohr magneton, e is the elementary charge, γ_0 is the gyromagnetic ratio, M_S is the saturation magnetization, and P is the current polarization.

We used a minimum discretization size of 1 nm. The implementation is conducted with the finite difference package mumax3.[41] Note that using a cell size larger than this value has a large effect on the critical field and currents for the DW motion, drastically changing its velocity. In order to avoid the appearance of a Joule heating that could damage the nanowire in an experimental set up,[42] we have considered the typical values of current densities reported in the literature in current-induced-dynamics experiments in nanowires (10^{11}–10^{12} A m^{-2}), restricting them to a maximum value of 5 × 10^{11} A m^{-2}. The micromagnetic parameters are presented in Table I, corresponding to a Ni nanowire.[43,44]

To track the BPDW dynamics, we follow both the axial component of the magnetization $m_x(t)$ and the BP position, which is determined by the intersection of three iso-surfaces ($m_x = 0$, $m_y = 0$, and $m_z = 0$).

III. CURRENT- INDUCED PROPAGATION OF A PRENUCLEATED BLOCH POINT DOMAIN WALL

The characteristic examples of the current-induced dynamics of a pre-nucleated head-to-head BPDW presented in Fig. 2 reveal a significant interplay between the Oersted field and the DW chirality. The panels in Figs. 2(b)–2(d) present results for currents applied in the positive (blue color) or negative (red color) direction along the nanowire axis. Importantly, this panel demonstrates the propagation of the BPDW in the direction opposite to the current (i.e., along the electron flow), irrespectively of the chirality of the Bloch point DW. The direction of the motion can be explained by analyzing the torques acting on the BPDW. This analysis shows that the propagation direction is defined by the $\vec{m}\times[\vec{m}\times\frac{\partial\vec{m}}{\partial x}]$ torque while a competition of the Oersted torque and the first term of the

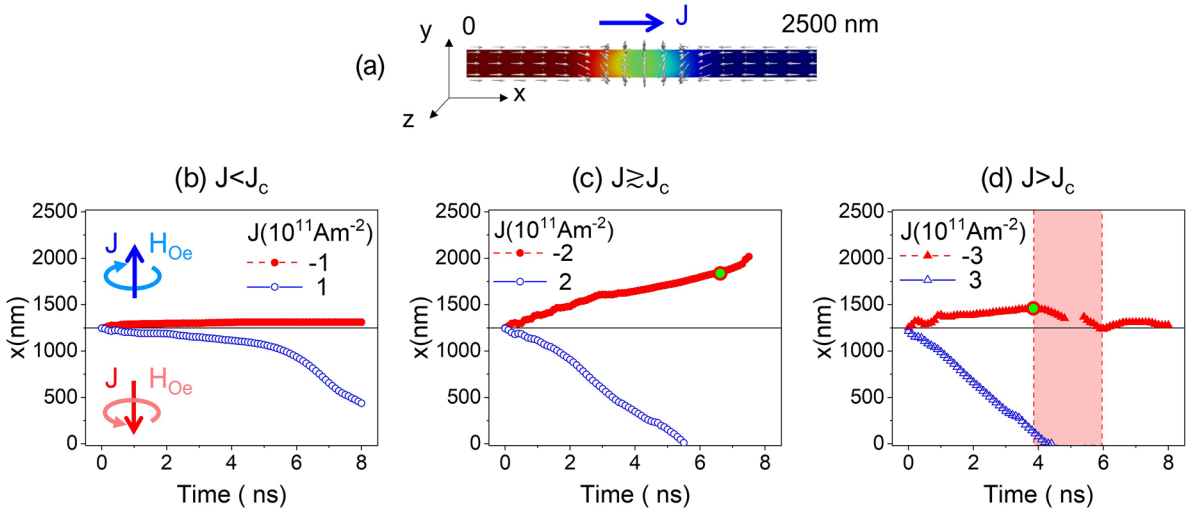

FIG. 2. (a) A head-to-head Bloch point wall driven by a spin-polarized current in a Ni nanowire. (b)–(d) The position of the Bloch point in the wire axis for three representative values of the current density. The blue lines show results for a BP domain wall with a "positive" chirality, i.e., with the curling sense coinciding with the Oersted field, while a red line denotes results for a domain wall with a "negative" chirality. Green points indicate the beginning of the chirality switching process of the Bloch point. The red shaded region is the interval of time where the BPDW switches its chirality, and the gap indicates the absence of the Bloch point.

spin transfer–torque produces a BP precession around the current direction.

A. Propagation and velocity of a Bloch point domain wall with "positive" chirality

A closer inspection of the current-induced dynamics given by the blue and red curves in Figs. 2(b)–2(d) demonstrates, respectively, that BPDWs having a "positive" chirality, i.e., the same sense of rotation than the Oersted field, propagate at faster speeds than those with chirality opposite to the Oersted field (called here "negative" chirality). Note the difference between the notion of "negative" chirality ("bad" chirality) or positive chirality ("good" chirality) used here with respect to that in field-induced dynamics,[11] where it is defined by the internal field (the sum of Zeeman and magnetostatic contributions).

In a BPDW driven by a positive current density (Fig. 3), the Oersted field has the same rotational direction than the DW, as indicated by the arrows sketched in the upper part of the figure. Figure 3(a) represents the magnetization on the nanowire surface. The inspection of the region depicted by yellow and cyan colors at 0.1 ns demonstrates a temporal widening of the domain wall [additionally highlighted in Fig. 3(c)] immediately after the activation of the current. The current triggers BPDW propagation in the direction opposite to it. In the first nanosecond the domain wall reaches a steady motion, as is shown by the blue curve in Fig. 2(d). Alternatively, Fig. 3(b) tracks the BP position (yellow circle). The iso-surface $m_x = 0$ (red color) represents the DW shape, which has a "butterfly"-like form and changes over time. The DW motion is accompanied by spin wave emission from the nanowire ends and the domain wall itself. The spin-wave emission from the wall is significantly larger in amplitude in the first nanosecond, during an accommodation of the DW structure to the Oersted field (see the available supplementary material video).

Note that, unlike previous reports on the BPDW dynamics under Oersted field and large damping value,[39] we did not observe any instability of the DW with a "positive" chirality. In the interval of investigated current densities we observed a steady propagation with relatively large velocities. Figure 4 summarizes the velocities reached by the BPDW with "positive" chirality for not too large current densities and far from the nanowire ends. The initial trend is a linear growth of the velocity with current densities up to 3×10^{11} A m^{-2}, above which a different slope is observed when increasing the current. This effect is frequently associated in the literature with the magnonic regime.[27,29,45] However, here the velocities are lower than the magnonic group velocity. We explain this effect through the increase of the DW width. Using dimensional analysis of the Zhang–Li torque we hypothesize that the velocity of the BP domain wall with "positive" chirality in steady regime is proportional to

$$\vec{v} \propto -\frac{(1+\xi\alpha)}{(1+\alpha^2)(1+\xi^2)} \frac{P\mu_B}{2e\gamma_o M_S} \left(\frac{D}{\Delta}\right) \vec{J}, \tag{2}$$

where D is the diameter of the nanowire and Δ is the BPDW width. Equation (2) reflects the fact that the propagation of BPDW is induced by the second term of the spin transfer torque in Eq. (1), and it occurs opposite to the direction of the current density as observed in the numerical model. Although the velocity is proportional to the current density, the increase of the domain wall width Δ at high Oersted fields partially compensates this effect, leading to a moderate increase in the DW speed observed for high currents in Fig. 4.

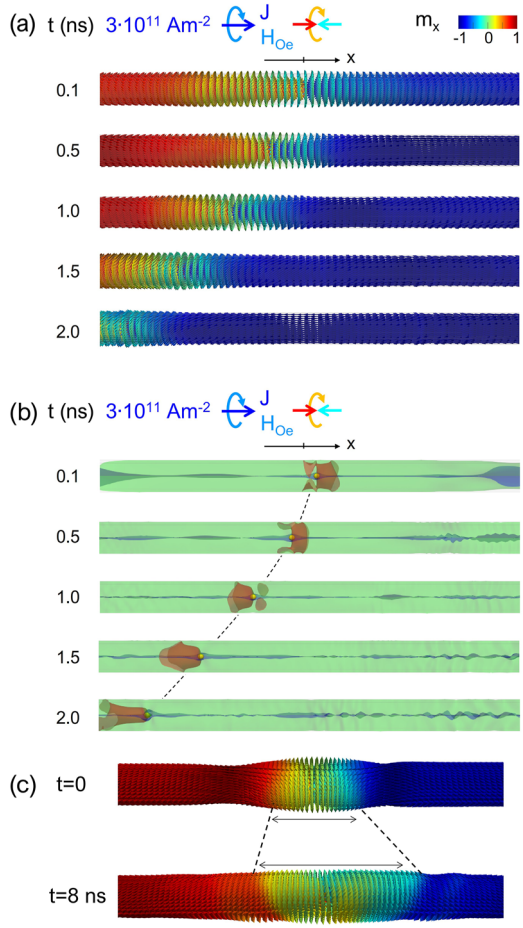

FIG. 3. Snapshots of the dynamics of a head-to-head Bloch point wall with "positive" chirality for a spin-polarized current of 3×10^{11} A m^{-2}. The azimuthal components of the Oersted field and the domain wall have the same orientation. (a) The surface magnetization is colored by the x-component. (b) Iso-surfaces of value m_x, m_y, and $m_z = 0$ are drawn in red, green, and blue, respectively. The BP is marked as a yellow sphere, and a dashed line in (b) indicates its propagation distance and direction. (c) Comparison of the DW width at initial and final moments.

B. Bloch point with "negative" chirality: Pinning, propagation, and chirality switching through BP annihilation and reinjection

For negative currents, the BPDW with the rotational sense depicted in Fig. 1 is of "negative" chirality. Figure 2 (red lines) shows three important regimes. For $J = -1 \times 10^{11}$ A m^{-2}, the BPDW does not propagate. For $J = -2 \times 10^{11}$ A m^{-2}, it propagates in the direction opposite to the current although with a velocity smaller than that observed for a DW with a "positive" chirality. Figure 2(d) evidences a complex dynamical process for $J = -3 \times 10^{11}$ A m^{-2}

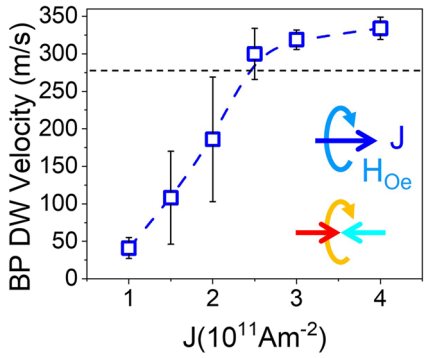

FIG. 4. The average velocity in the steady regime far from the ends of the nanowire of BP DW with "positive" chirality, as a function of applied current density. The dashed line schematically delimits two regimes of propagation.

that encompasses two well defined regions divided by the red interval.

In contrast to BPDWs driven by positive currents, where BP propagates always along the nanowire axis until reaching the ends, for $J = -3 \times 10^{11}$ A m^{-2}, the BP deviates from the nanowire axis toward the surface, leading to the BP ejection and chirality switching, in line with Ref. 37. Green dots in Fig. 2(d) indicate the start of a chirality switching process. This is characterized by a change in the slope of the red curve (i.e., an acceleration process). The red interval indicates a void of any Bloch point in the entire wire, and thereby the annihilation of the original BP at t = 4.5 ns, followed by the later creation of a new BPDW with opposite chirality, as presented in Figs. 5(a) and 5(b). See also the available supplementary material video.

A more detailed representation of the chirality switching is shown in Fig. 5(c), illustrating the change of the azimuthal magnetization component (initially in red color) to the opposite direction (blue color). It also demonstrates the complexity of the transformation dynamics with an intermediate formation of the VAVDW, visible at 2.0–3.5 ns.

Strikingly, notice in Fig. 5 that the propagation of the BP is either in the direction of the current or opposite to it during the transformation process, and notice the injection of a new BP with "positive" chirality. The structure of the injected BP is deformed by the Oersted field and Zhang–Li torque as evidenced by the red isosurface at t = 8 ns. This BP first moves in the direction parallel to the current but then returns to a position close to the initial one. What is striking about the overall process is that the chirality change is not followed by a propagation of the new BPDW that now has a "positive" chirality, but results in a DW stopping. This was confirmed by integration of the dynamics for longer times up to 20 ns. The mechanism of this effect is the following. Even prior to the DW instability, the Oersted field creates a chiral magnetization with direction parallel to it along the whole nanowire dynamically, starting from the nanowire ends.[39] The interaction between this chiral magnetization with a BPDW having the opposite sense creates two *quasi* DWs [on both sides of the BP, as visible in blue in Fig. 5(b)]. At 1 ns, the BPDW is surrounded by these domain walls. The whole structure is quite stable and topologically protected and cannot efficiently annihilate, impeding the propagation of the central BPDW (even after its transformation). This also explains the pinned or the slow motion for lower current densities shown in Figs. 2(b) and 2(c). At high current densities, after the BPDW chirality switching, a part of this structure is annihilated through spin wave emission. However, the remaining structure is quite complex and still contains the reminiscence of the encounter between quasi DWs and the BPDW with opposite chiralities (compare the structures in Fig. 5 at 0.1 and 8 ns and also with those in Fig. 3 at 1 ns). We believe that this constitutes a new DW pinning mechanism, produced mainly by the action of the Oersted field.

IV. CURRENT- INDUCED DYNAMICS OF A VORTEX–ANTIVORTEX DOMAIN WALL

A vortex–antivortex DW is an alternative domain wall that is formed in cylindrical nanowires. Research on MCNWs with large diameters has mainly focused on domain walls of the BP type rather than on the vortex–antivortex domain wall.[11,27,37,38,46,47] A vortex–antivortex domain wall has a slightly larger energy than a Bloch point domain wall.[35] However, simulations indicate that the former wall is more easily formed in magnetic nanowires[35,38] than the BP domain wall. The structure and topology of this wall, depicted in Figs. 1(b), 1(c), and 8(a), differ from the Bloch point and so its dynamics under magnetic fields. So far, little attention has been paid to its dynamics under spin-polarized current. In Fig. 6, we present results on the current-induced dynamics of a pre-nucleated VAVDW (followed by the average magnetization component along the nanowire) for different current densities.

For low currents such as those in Figs. 6(b) and 6(c), the VAVDW does not propagate, or the propagation is of the order of a few nanometers during the accommodation to the Oersted field, after which the domain wall stops. Starting from $J = -1.5 \times 10^{11}$ A m^{-2}, we have observed that this prenucleated stable VAVDW suffers in approximately a fraction of 1 ns a transformation into a BPDW with the same circulation as the Oersted field, i.e., with the "positive" chirality. The resulting position of the BPDW as a function of time is presented in Figs. 6(g)–6(j). The transformation time is smaller for positive currents, which is interesting for the development of ultrafast spintronic applications (see the supplementary material). The dynamic process differs considerably from the chirality change of the BPDW in Fig. 2(d). It also differs from the transformation of the BPDW into a VAVDW described by De Riz *et al.*[37] in nanowires with smaller radii, where the change starts and ends in BPDW, and at certain stage of the process, the magnetic configuration resembles an excited (unstable) VAVDW, and thus not a metastable VAVDW per se.

Importantly for the development of spintronic applications with low power consumption, the transformation of a VAVDW into a BPDW requires a small critical current, $|J| = 1.0 \times 10^{11}$ A m^{-2}, three times lower than that for the chirality switching in our study, 10 times lower than the values reported in Ref. 37 and six times lower than the current required for chirality switching of BPDW created at the nanowire ends.[39,37]

By the same Oersted-field induced pinning effect, the propagation of a new BPDW may be either slow or almost null. For certain current densities, domain walls may remain pinned at the

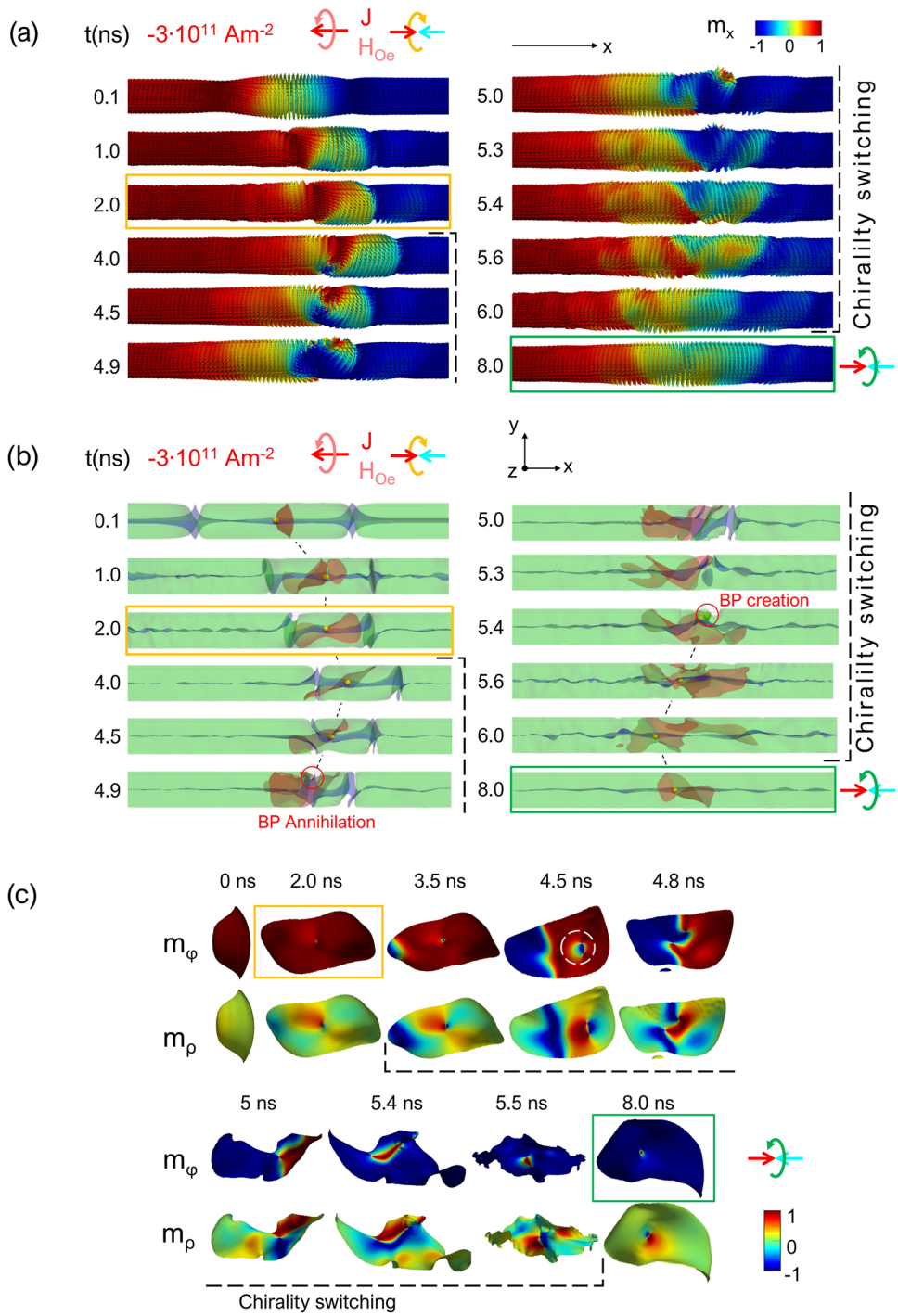

FIG. 5. (a) Snapshots of the dynamics of a head-to-head Bloch point wall with "negative" chirality for a spin-polarized current of -3×10^{11} A m^{-2}. The azimuthal components of the Oersted field and the domain wall have opposite orientations at t = 0. Initially, the DW slowly propagates in the direction opposite to the current. Between 3.5 and 5.4 ns, it switches its chirality to accommodate to the sense of the Oersted field. (a) Snapshots of the surface magnetization parallel to the nanowire axis. (b) Iso-surfaces of values m_x, m_y, and $m_z = 0$ are drawn in red, green, and blue, respectively. The Bloch point is marked as a yellow sphere, and the dashed line in (b) indicates its propagation distance and direction. (c) Enlarged snapshots of the part of the isosurface of value $m_x = 0$ that contains the Bloch Point domain wall with "negative" chirality during the first 8 ns for a spin-polarized current of -3×10^{11} A m^{-2}. Colors in the first and second row indicate the values of the azimuthal and radial components of the magnetization, respectively. The switching of chirality occurs between t = 3.5 ns and t = 5.5 ns.

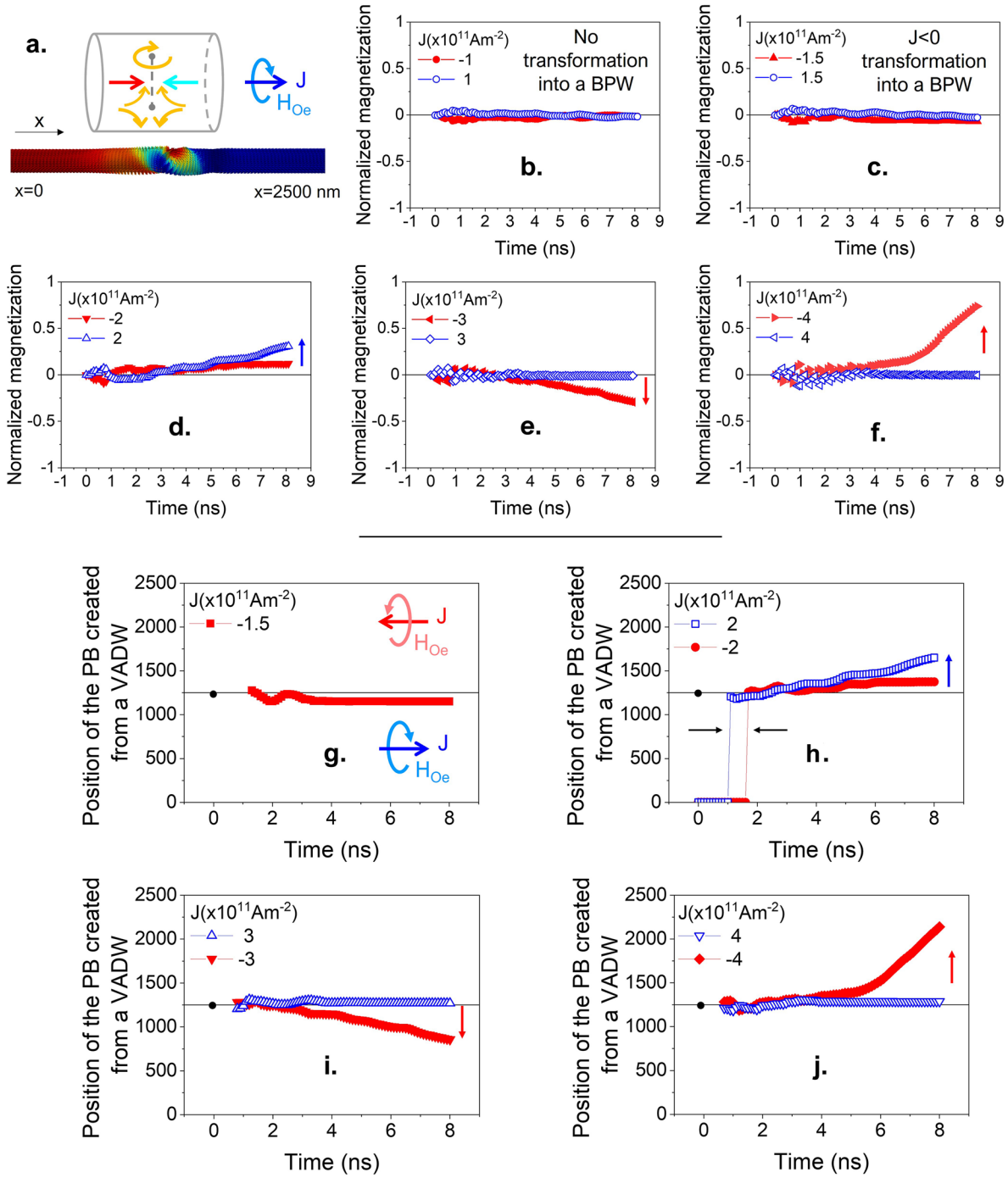

FIG. 6. (a) A sketch of a head-to-head vortex–antivortex domain wall driven by a spin-polarized current in a Ni nanowire. [(b)–(f)] Magnetization dynamics of the VAVDW followed by the longitudinal magnetization along the nanowire axis for a selection of current densities. (g)–(j) Position as a function of time of the BPDW injected after the transformation from the vortex–antivortex domain wall for different current values. t = 0 corresponds to the injection moment.

center of the nanowire after the transformation into a BPDW and accommodation to the Oersted field. Importantly and contrary to expectations, Figs. 6(d)–6(f) indicate that the BPDW created from this VAVDW in the nanowire may propagate a large distance in the direction of the current ($J = -3 \times 10^{11}$ A m^{-2}) or opposite to it ($J = -4 \times 10^{11}$ A m^{-2}).

Figure 7 provides an example of the domain wall transformation for $J = -3 \times 10^{11}$ A m^{-2}, where the domain wall moved

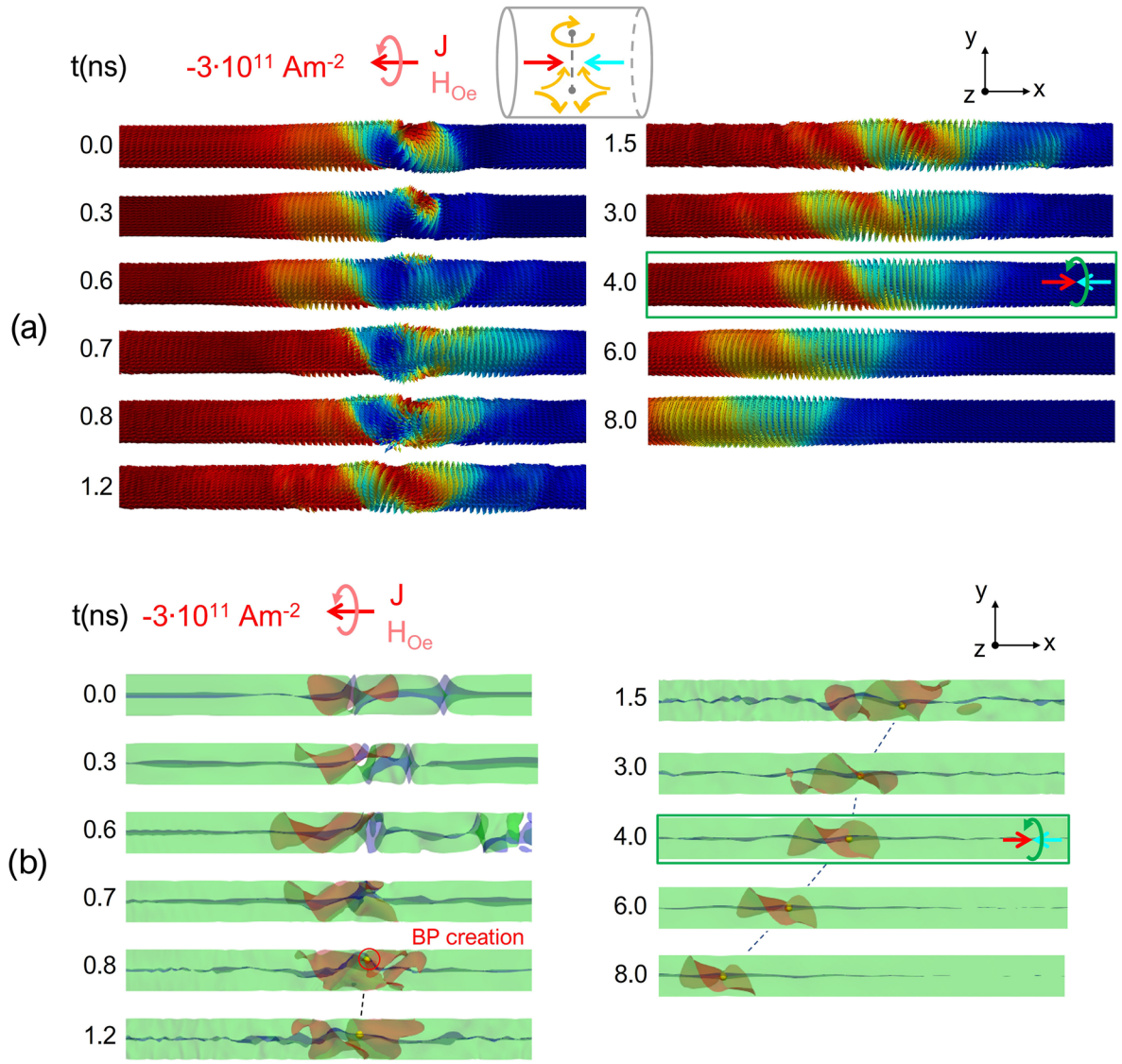

FIG. 7. (a) Snapshots of the dynamics of a head-to-head vortex–antivortex domain wall (surface magnetization) for a current of -3×10^{11} A m^{-2}. (b) Dynamics of isosurfaces of values m_x, m_y, and $m_z = 0$ are drawn in red, green, and blue, respectively. The Bloch point is marked as a yellow sphere, and the dashed line in (b) indicates its propagation distance and direction. Between 0 and 1.2 ns, the VADW transforms into a BP DW with "positive" chirality.

along the current direction (i.e., opposite to the electron flow). Immediately after the switching of the current pulse, the Oersted field induces torques with opposite orientations on the magnetization at the surface of the structure, triggering an expansion of the domain wall and a rotation of the vortex–antivortex pair on the surface in the timeframe between t = 0 and t = 0.8 ns. At t = 0.8 ns, the vortex–antivortex pair is annihilated on the surface and the magnetization begins a gradual alignment into the direction of the Oersted field, accompanied by a spin wave emission that lasts for nanoseconds. Importantly, from t = 0.8 ns, a BPDW with "positive" chirality is already visible and starts moving. See also the supplementary material (video). In order to illustrate the propagation of this BPDW, the dynamics of zero value isosurfaces of the magnetization components in the nanowire are depicted in Fig. 7(b). The two "hills" in the blue isosurface in Fig. 7(b) at t = 0 indicate that the Oersted field induced three regions with alternating orientation of the m_ϕ component so that the middle region has a chirality opposite to that of the Oersted field. This region is gradually compressed by the neighboring ones, which have the chirality of the Oersted field. After 0.8 ns, the middle region is annihilated with a simultaneous injection of a Bloch point on the surface at the intersection with the red isocurve. In the following nanoseconds, the Bloch point

approaches the axis of the nanowire without reaching it and keeps precessing around this axis and slightly oscillates back and forth. During this process, the BP begins to propagate in the direction of the current, while not fully centered in the axis of the nanowire. An inspection of the Bloch point injected at -4×10^{11} A m^{-2} resulting in a DW propagation opposite to the current direction (Fig. 8) confirms that in this case the transformation occurs similarly to that in Fig. 7, and in both cases the Bloch points have identical chirality.

An important open question is why the BPDWs with a "positive" chirality created by the transformation from initial VAVDW propagates large distances in either one or the other direction. We have observed that although the injection of the BP may occur with a component of velocity parallel/antiparallel to the current direction, the resulting BPDW may propagate in any direction, independently on the initial velocity. Additionally, the BP precession around the axis of the nanowire shows a gyrotropic motion. We can hypothesize a possible role of an initial angular momentum that, as the DW is chiral in nature, can define the propagation direction. Additionally, one can assume the possibility that the BP domain wall motion possesses some inertia. Indeed, an inertial mass has been previously evaluated for Bloch lines in ferromagnets with high quality factor.[47] The precession of the BP around the axis of the nanowire continues for a considerable time, with simultaneous spinwave emission as a mechanism of releasing energy and angular momentum, in contrast to prenucleated BPs. The spin wave spectrum in cylindrical systems is expected to be non-reciprocal in a chiral background,[48]

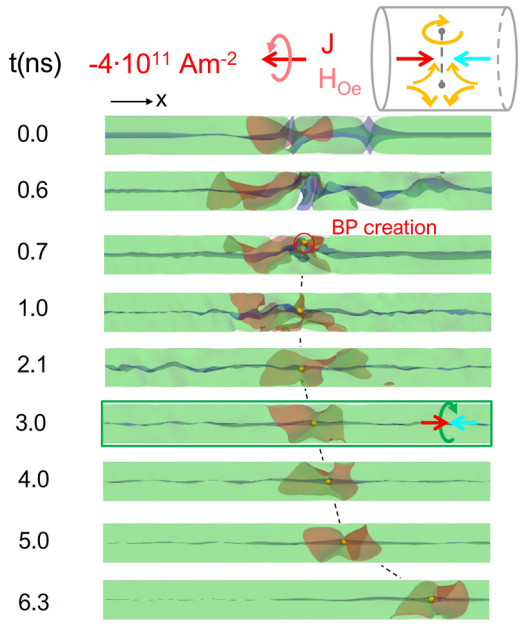

FIG. 8. Snapshots of the dynamics of a head-to-head vortex–antivortex domain wall for a spin-polarized current of -4×10^{11} A m^{-2}. Isosurfaces of values m_x, m_y, and $m_z = 0$ are drawn in red, green, and blue, respectively. The Bloch point is marked as a yellow sphere. Between 0 and 1.2 ns, the VADW transforms into a BPW with "positive" chirality. The dashed line indicates the DW propagation distance and direction.

and, therefore, one may also expect a net magnonic current that may exert an additional torque on a BPDW.

V. CONCLUSIONS

Our results show that domain wall propagation in cylindrical magnetic nanowires has a high complexity due to their chiral nature. We have observed a plethora of behaviors that would critically affect the manipulation and control of DWs as information carriers in magnetic recording and spintronic technologies based on CMNWs.

Importantly, BP domain walls with circular magnetization direction parallel to the Oersted field can be stable and propagate in large distances in the direction opposite to the current with reasonably high velocities, comparable to the best values in stripes. According to recent reports on nanowires with Oersted field only and high damping value, BPDWs become unstable after a certain current density.[37] We have observed this instability only for BPDWs with "negative" chirality (i.e., with circular magnetization direction antiparallel to Oersted field) in nanowires with a low damping. However, we have shown that, at large current densities, the velocities are slowed down, and we attribute this effect to the increase of DW width due to Oersted field influence.

In current experimental situations, there is no straightforward way to control DW chirality and its type, neither it is easy *a priori* to determine its characteristics. In general, our results show that, in most situations, an arbitrary DW will transform into a BPDW with chirality with the azimuthal magnetization component parallel to the Oersted field. A main consequence is therefore the reduction of the number of possible spin textures to be controlled in devices based on nanowires. However, unlike an initial DW with a "positive" chirality, the transformed domain wall does not experience a steady propagation. The resulting BPDW can be pinned by the action of the current (through the Oersted field) or may propagate either along the current direction or opposite to it. In the first case, we have identified a novel pinning mechanism, due to the action of the Oersted field, which would act on a BPDW with initial chirality opposite to its rotational sense. In the latter case, we have shown that the BPDW created from the transformation of the VAVDW can propagate in either direction. We attribute this effect to the fact that the BP initial inertia (angular momentum and/or effective mass) may play a key role in the dynamics of the BPDW. This dynamical effect has not been considered so far.

These findings raise intriguing questions regarding the nature and extent of the influence of the chirality, angular momentum, and inertia in the manipulation and control of chiral DWs. On one hand, these effects highlight a fundamental interplay of chirality and dynamics. On the other hand, they will be critical for the development of technologies based on magnetic cylindrical nanowires, such as magnetic recording applications based on 3D racetrack memory or Bloch point-based spintronics.

SUPPLEMENTARY MATERIAL

The supplementary online material is a video that contains supplementary material and several examples of dynamics of Bloch point domain walls, vortex–antivortex domain walls, and their dynamical transformations.

ACKNOWLEDGMENTS

This work was supported by the Ministry of Science and Innovation MCIN/AEI/10.13039/501100011033 (Grant Nos. PID2019-108075RB-C31 and PID2019-108075RB-C32). J.A.F.-R. acknowledges the support of the Alexander von Humboldt Foundation.

AUTHOR DECLARATIONS

Conflict of Interest

The authors have no conflicts to disclose.

Author Contributions

J. A. Fernandez-Roldan: Conceptualization (equal); Formal analysis (equal); Investigation (equal); Methodology (equal); Resources (equal); Software (equal); Supervision (equal); Validation (equal); Visualization (equal); Writing – original draft (equal); Writing – review & editing (equal). **O. Chubykalo-Fesenko**: Conceptualization (equal); Formal analysis (equal); Investigation (equal); Methodology (equal); Resources (equal); Software (equal); Supervision (equal); Validation (equal); Visualization (equal); Writing – original draft (equal); Writing – review & editing (equal).

DATA AVAILABILITY

The data that support the findings of this study are available from the corresponding author upon reasonable request.

REFERENCES

[1] A. Fernández-Pacheco, R. Streubel, O. Fruchart, R. Hertel, P. Fischer, and R. P. Cowburn, Nat. Commun. **8**, 15756 (2017).
[2] R. Streubel, P. Fischer, F. Kronast, V. P. Kravchuk, D. D. Sheka, Y. Gaididei, O. G. Schmidt, and D. Makarov, J. Phys. D: Appl. Phys. **49**, 363001 (2016).
[3] C. Donnelly, A. Hierro-Rodríguez, C. Abert, K. Witte, L. Skoric, D. Sanz-Hernández, S. Finizio, F. Meng, S. McVitie, J. Raabe, D. Suess, R. Cowburn, and A. Fernández-Pacheco, Nat. Nanotechnol. **17**, 136 (2022).
[4] D. Sanz-Hernández, A. Hierro-Rodriguez, C. Donnelly, J. Pablo-Navarro, A. Sorrentino, E. Pereiro, C. Magén, S. McVitie, J. M. de Teresa, S. Ferrer, P. Fischer, and A. Fernández-Pacheco, ACS Nano **14**, 8084 (2020).
[5] J. García, J. A. Fernández-Roldán, R. González, M. Méndez, C. Bran, V. Vega, S. González, M. Vázquez, and V. M. Prida, Nanomaterials **11**, 3077 (2021).
[6] J. Marqués-Marchán, J. A. Fernandez-Roldan, C. Bran, R. Puttock, C. Barton, J. A. Moreno, J. Kosel, M. Vazquez, O. Kazakova, O. Chubykalo-Fesenko, and A. Asenjo, Nanomaterials **12**, 1968 (2022).
[7] E. Berganza, J. Marqués-Marchán, C. Bran, M. Vazquez, A. Asenjo, and M. Jaafar, Materials **14**, 5671 (2021).
[8] C. Bran, J. A. Fernandez-Roldan, R. P. Del Real, A. Asenjo, O. Chubykalo-Fesenko, and M. Vazquez, Nanomaterials **11**, 600 (2021).
[9] P. Fischer, D. Sanz-Hernández, R. Streubel, and A. Fernández-Pacheco, APL Mater. **8**, 010701 (2020).
[10] D. D. Sheka, Appl. Phys. Lett. **118**, 230502 (2021).
[11] R. Hertel, Spin **03**, 1340009 (2013).
[12] O. V. Pylypovskyi, D. D. Sheka, V. P. Kravchuk, K. v. Yershov, D. Makarov, and Y. Gaididei, Sci. Rep. **6**, 23316 (2016).
[13] E. Y. Vedmedenko, R. K. Kawakami, D. D. Sheka, P. Gambardella, A. Kirilyuk, A. Hirohata, C. Binek, O. Chubykalo-Fesenko, S. Sanvito, B. J. Kirby, J. Grollier, K. Everschor-Sitte, T. Kampfrath, C.-Y. You, and A. Berger, J. Phys. D: Appl. Phys. **53**, 453001 (2020).
[14] E. Berganza, J. A. Fernandez-Roldan, M. Jaafar, A. Asenjo, K. Guslienko, and O. Chubykalo-Fesenko, Sci. Rep. **12**, 3426 (2022).
[15] S. Gliga, G. Seniutinas, A. Weber, and C. David, Mater. Today **26**, 100 (2019).
[16] D. Makarov, O. M. Volkov, A. Kákay, O. v. Pylypovskyi, B. Budinská, and O. v. Dobrovolskiy, Adv. Mater. **34**, 2101758 (2022).
[17] J. A. Fernandez-Roldan, R. Perez del Real, C. Bran, M. Vazquez, and O. Chubykalo-Fesenko, Nanoscale **10**, 5923 (2018).
[18] E. Berganza, M. Jaafar, J. A. Fernandez-Roldan, M. Goiriena-Goikoetxea, J. Pablo-Navarro, A. García-Arribas, K. Guslienko, C. Magén, J. M. de Teresa, O. Chubykalo-Fesenko, and A. Asenjo, Nanoscale **12**, 18646 (2020).
[19] C. Andreas, A. Kákay, and R. Hertel, Phys. Rev. B **89**, 134403 (2014).
[20] S. Da Col, S. Jamet, N. Rougemaille, A. Locatelli, T. O. Mentes, B. S. Burgos, R. Afid, M. Darques, L. Cagnon, J. C. Toussaint, and O. Fruchart, Phys. Rev. B **89**, 180405 (2014).
[21] A. Wartelle, B. Trapp, M. Staňo, C. Thirion, S. Bochmann, J. Bachmann, M. Foerster, L. Aballe, T. O. Menteş, A. Locatelli, A. Sala, L. Cagnon, J.-C. Toussaint, and O. Fruchart, Phys. Rev. B **99**, 024433 (2019).
[22] C. Bran, E. Saugar, J. A. Fernandez-Roldan, R. P. Del Real, A. Asenjo, L. Aballe, M. Foerster, A. Fraile Rodríguez, E. M. Palmero, M. Vazquez, and O. Chubykalo-Fesenko, Nanoscale **13**, 12587 (2021).
[23] S. Da Col, S. Jamet, M. Staňo, B. Trapp, S. Le Denmat, L. Cagnon, J. C. Toussaint, and O. Fruchart, Appl. Phys. Lett. **109**, 062406 (2016).
[24] C. Bran, J. A. Fernandez-Roldan, R. P. Del Real, A. Asenjo, Y.-S. Chen, J. Zhang, X. Zhang, A. Fraile Rodríguez, M. Foerster, L. Aballe, O. Chubykalo-Fesenko, and M. Vazquez, ACS Nano **14**, 12819 (2020).
[25] C. Bran, E. Berganza, J. A. Fernandez-Roldan, E. M. Palmero, J. Meier, E. Calle, M. Jaafar, M. Foerster, L. Aballe, A. Fraile Rodriguez, R. P. Del Real, A. Asenjo, O. Chubykalo-Fesenko, and M. Vazquez, ACS Nano **12**, 5932 (2018).
[26] N. L. Schryer and L. R. Walker, J. Appl. Phys. **45**, 5406 (1974).
[27] R. Hertel, J. Phys.: Condens. Matter **28**, 483002 (2016).
[28] M. Yan, A. Kákay, S. Gliga, and R. Hertel, Phys. Rev. Lett. **104**, 057201 (2010).
[29] X.-P. Ma, J. Zheng, H.-G. Piao, D.-H. Kim, and P. Fischer, Appl. Phys. Lett. **117**, 062402 (2020).
[30] M. Schöbitz, S. Finizio, A. de Riz, J. Hurst, C. Thirion, D. Gusakova, J. C. Toussaint, J. Bachmann, J. Raabe, and O. Fruchart, Appl. Phys. Lett. **118**, 172411 (2021).
[31] R. Wieser, U. Nowak, and K. D. Usadel, Phys. Rev. B **69**, 064401 (2004).
[32] Y. P. Ivanov, A. Chuvilin, S. Lopatin, H. Mohammed, and J. Kosel, ACS Appl. Mater. Interfaces **9**, 16741 (2017).
[33] E. M. Palmero, C. Bran, R. P. Del Real, and M. Vázquez, Nanotechnology **26**, 461001 (2015).
[34] H. Forster, T. Schrefl, W. Scholz, D. Suess, V. Tsiantos, and J. Fidler, J. Magn. Magn. Mat. **249**, 181 (2002).
[35] C. A. Ferguson, D. A. MacLaren, and S. McVitie, J. Magn. Magn. Mater. **381**, 457 (2015).
[36] S. Jamet, N. Rougemaille, J. C. Toussaint, and O. Fruchart, in *Magnetic Nano- and Microwires*, edited by M. Vázquez (Woodhead Publishing, 2015), pp. 783–811.
[37] A. De Riz, J. Hurst, M. Schöbitz, C. Thirion, J. Bachmann, J. C. Toussaint, O. Fruchart, and D. Gusakova, Phys. Rev. B **103**, 054430 (2021).
[38] R. Moreno, V. L. Carvalho-Santos, D. Altbir, and O. Chubykalo-Fesenko, J. Magn. Magn. Mater. **542**, 168495 (2022).
[39] J. A. Fernandez-Roldan, R. P. Del Real, C. Bran, M. Vazquez, and O. Chubykalo-Fesenko, Phys. Rev. B **102**, 024421 (2020).
[40] M. Schöbitz, A. De Riz, S. Martin, S. Bochmann, C. Thirion, J. Vogel, M. Foerster, L. Aballe, T. O. Menteş, A. Locatelli, F. Genuzio, S. Le-Denmat, L. Cagnon, J. C. Toussaint, D. Gusakova, J. Bachmann, and O. Fruchart, Phys. Rev. Lett. **123**, 217201 (2019).
[41] A. Vansteenkiste, J. Leliaert, M. Dvornik, M. Helsen, F. Garcia-Sanchez, and B. Van Waeyenberge, AIP Adv. **4**, 107133 (2014).
[42] M. P. Proenca, M. Muñoz, I. Villaverde, A. Migliorini, V. Raposo, L. Lopez-Diaz, E. Martinez, and J. L. Prieto, Sci. Rep. **9**, 17339 (2019).

[43]Y. P. Ivanov, M. Vázquez, and O. Chubykalo-Fesenko, J. Phys. D: Appl. Phys. **46**, 485001 (2013).
[44]J. A. Fernandez-Roldan, Y. P. Ivanov, and O. Chubykalo-Fesenko, *Magnetic Nano- and Microwires*, 2nd ed. (Woodhead Publishing, 2020), Chap. XIV, Vol. 403, ISBN: 9780081028322.
[45]M. Yan, A. Kákay, C. Andreas, and R. Hertel, Phys. Rev. B **88**, 220412 (2013).
[46]J. Hurst, A. De Riz, M. Staňo, J. C. Toussaint, O. Fruchart, and D. Gusakova, Phys. Rev. B **103**, 024434 (2021).
[47]Y. A. Kufaev and E. B. Sonin, "Dynamics of a Bloch point (point soliton) in a ferromagnet," J. Experim. Theoret. Phys. **68**, 879 (1989).
[48]J. A. Otálora, M. Yan, H. Schultheiss, R. Hertel, and A. Kákay, Phys. Rev. Lett. **117**, 227203 (2016).